Advanced Powder Technology 35 (2024) 104305

Contents lists available at ScienceDirect

Advanced Powder Technology

journal homepage: www.elsevier.com/locate/apt

Effect of ultrasonication on rising characteristics of a single gas bubble

Yannan Liang [1], Hainan Wang [1], Ruoqian Zhou, Danlong Li, Haijun Zhang *

Chinese National Engineering Research Center of Coal Preparation and Purification, China University of Mining and Technology, Xuzhou 221116, Jiangsu, China
School of Chemical Engineering and Technology, China University of Mining and Technology, Xuzhou 221116, Jiangsu, China

ARTICLE INFO

Article history:
Received 24 June 2023
Received in revised form 14 November 2023
Accepted 10 December 2023

Keywords:
Flotation
Gas bubble
Ultrasonication
Aspect ratio
Rising velocity

ABSTRACT

In recent years, ultrasonication has been used to enhance flotation process. Gas bubble is the unique carrier during mineral flotation, and thus its characteristics play an important role. However, the bubble rising characteristics under ultrasound action are not clear. Therefore, this paper aims to investigate the effect of ultrasonication on bubble rising behaviors in deionized water and MIBC (Methyl Isobutyl Carbinol) solution. A laboratory visualization system of bubble motion with ultrasonication was designed based on the high-speed dynamic video technology to record the bubble rising process and analyze bubble rising characteristics. Bubble aspect ratio was found to increase with the surfactant concentration increasing, but the rising velocity was in opposite state. In each solution, a significantly higher bubble sphericity was observed with ultrasonication than that without ultrasonication, conversely, the bubble rising velocity was smaller under the action of ultrasonication. A roughly negative linear relationship was found between the bubble shape and rising velocity, and the ultrasonication diminished this relationship. Marangoni effect was considered as the cause of MIBC affecting the bubble motion, and possible explanations of ultrasonication affecting the bubble motion were given from the perspective of bubble surface wave, cavitation bubble oscillation and sound radiation force.

1. Introduction

Froth flotation has been widely used in mineral separation, water treatment and waste plastics recycling [1–3]. During the flotation process, after the bubble-particle collision, hydrophobic particles adhering to bubbles are transferred towards the froth layer to form concentrates, and hydrophilic particles remain in the flotation cell to form tailings [4]. The comprehensive effect of partial-bubble collision, attachment and detachment affects the flotation rate and flotation recovery [5,6]. As the carrier, bubble characteristics play an important role in the flotation process [7].

Extensive studies have been carried out on bubble behaviors, including bubble size, shape, and velocity. In the flotation process, the bubble size is mainly affected by the slurry property and the mechanical energy input. The solution surface tension is an essential factor affecting the bubble size, and the slurry surface tension can be changed by adding surfactants. Cho and Laskowski [8] studied the frother influence on the bubble size in a mechanical stirring flotation cell. The results showed that the bubble size decreased rapidly with the increase in frother concentrations until the critical coalescence concentration (CCC). The bubble size became constant when the frother concentration exceeded the CCC value. Frothers have different effects on surface tension due to their other chemical groups, chain length, and solubility [9,10]. Additionally, it was found that the surface tension decreased with an increase of the slurry temperature, which significantly reduced the bubble size [11]. The slurry pH affects the bubble surface electrical properties, and thus the bubble size. Alam et al. [12] evaluated the effect of pH on bubble size during electro-flotation. They found that the average bubble size of H_2 in a neutral environment was smaller than that of H_2 in a strongly acidic or strongly alkaline environment. A systematic review of bubble size regulation was performed by Wang et al. [4]. The mechanical energy input promotes the collision of turbulent vortices and gas bubbles, which leads to bubble deformation and rupture. Moreover, the gas bubble can even be broken into two or more small gas bubbles in low flow rates, thus reducing the bubble size [13,14]. Most of the studies related to the bubble shape and velocity were focused on solution environment. Many scholars have studied the influence of frother on bubble rising characteristics and found that bubble aspect ratio and rising velocity increased and decreased with increasing concentration,

* Corresponding author at: Chinese National Engineering Research Center of Coal Preparation and Purification, China University of Mining and Technology, Xuzhou 221116, Jiangsu, China.
E-mail address: zhjcumt@163.com (H. Zhang).
[1] These authors contributed equally to this work.

https://doi.org/10.1016/j.apt.2023.104305

respectively, and salts show a similar ability [15–17]. Zhu et al. [18] studied the effect of dodecylamine (DDA)-frother blend on bubble rising characteristics, it was found that DDA addition had a significant effect on further increasing the aspect ratio and decreasing the rising velocity of gas bubbles compared to individual MIBC and 2-octanol solutions. Moreover, Maldonado et al. [17] found a unique relationship between the bubble shape and rise velocity, specifically, flattened bubbles lead to a high rising velocity, while spherical bubbles exhibit a low velocity. Yan et al. [19,20] studied the rising motion of single gas bubbles in deionized water and surfactant solutions and found periodic fluctuations in the bubble terminal velocity, indicating a nonconstant bubble drag.

Recently, ultrasonication has been introduced into flotation and significantly improved flotation performance [21,22]. The influence of ultrasonication on flotation bubbles is receiving increasing attention. Wang et al. and Ozkan, S. G. [23,24] found that a specific frequency of ultrasonic irradiation could decrease the dimensionality of gas bubbles, and the gas bubbles became more stable. Yasmin et al. and Yang et al. [25,26] studied the bubble volume resonance under ultrasonication. When the acoustic field with low sound intensity was active, the bubble underwent radial linear vibration (volume mode), and the oscillatory motion of the bubble exhibited periodic radial expansion and contraction behavior around a certain average value. Gao et al. [27] found that the size of bubbles increased with the thickness of the vibrating plate of the ultrasonic transducer due to the aggregation of bubbles under the influence of ultrasound. When the acoustic pressure is between the transient cavitation threshold and the rectified diffusion threshold, the gas nuclei in the water or on the particle surface will grow without collapsing. Massive cavitation bubbles form due to their diffusion and coalescence [28,29]. Mao et al. [30,31] studied the effect of standing wave field on flotation bubbles, and the results showed that bubbles aggregated in the pulp when the ultrasound was turned on. Bubbles would aggregate at the pressure nodes or antinodes due to both the primary and secondary bjerknes forces in standing wave field.

However, most of the effects of ultrasound on bubbles are focused on bubble volume or cavitation bubbles. The gas bubble characteristics (bubble shape, trajectory, and velocity) as they gradually fade into the sound field are relatively few. It is worth noting that there are significant differences between cavitation bubbles and gas bubbles. Cavitation bubbles are the bubbles appear at the time the hydraulic pressure drops below the vapor pressure of the water. The gas bubbles are the bubbles generated by gas gathering. In this work, gas bubbles were formed by pushing gas into the solution through a syringe. The cavitation bubble volume is usually small and its buoyancy is usually negligible. Differently, buoyancy is an important external force for bubble, which causes the bubble deformation and motion [32]. During the ultrasonic flotation process, cavitation bubbles mostly coexist with gas bubbles, and the effect of ultrasound on gas bubble characteristics should not be neglected. The aim of this study is to investigate the effect of ultrasonication on bubble rise characteristics. A high-speed camera (i-SPEED 3) and Image Pro Plus were used to record and analyze the bubble rising characteristics, respectively. And the mechanism of ultrasound effect on bubble characteristics will be discussion.

2. Experimental

2.1. System and reagent

This investigation was conducted using a laboratory visualization system of bubble movement with ultrasonication, as shown in Fig. 1. It mainly consists of five components: (1) a customized

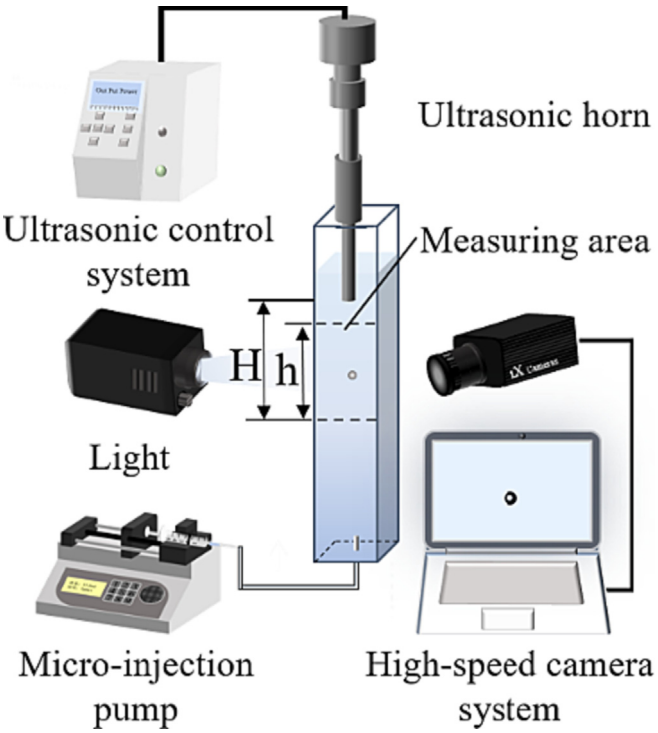

Fig. 1. Schematic diagram of the laboratory visualization system of bubble movement with ultrasonication.

rectangle plexiglass observation tank of 5 cm width, 5 cm depth and 25 cm height, (2) a LSP02-1B precision syringe pump (Longer Precision Pump Co., Ltd., China), (3) a light source, (4) an I-Speed 230 high-speed camera (iX Cameras Ltd., UK), and (5) an FS-900 N ultrasonic device (Shanghai Shengxi Ultrasonic Instrument Co., Ltd., China) consisted of an ultrasonic horn and an ultrasound generator. A stainless-steel capillary orifice with an inner diameter of 0.7 mm, which is fixed with the precision syringe pump, is inserted into the bottom of the observation tank. The size of generated gas bubble is regulated using controlling the injection speed of the precision syringe pump. A high-speed camera and a light source are placed on the front and rear sides of the observation slot, respectively. A measuring area with 5 cm of width and 8 cm of height is used to record the bubble rising process (h is 8 cm), and the bottom of it is 10 cm away from the ultrasonic horn tip (H is 10 cm). In addition, deionized water with a resistivity of 18.25 MΩ/cm was used throughout the experiments, and the surfactant was methyl isobutyl carbinol (MIBC) obtained from Shanghai Aladdin Biochemical Technology Co., Ltd.

2.2. Measurement of bubble rising characteristics

In the measurement of bubble rising characteristics, a single gas bubble of 2.6 mm diameter was generated at the exit of a stainless-steel capillary orifice. The flow of the micro-injection pump was set as 5 μL/min. In addition, the operating frequency and input power of the ultrasonic device were set as 20 kHz and 90 W, respectively. Bubble rising process in the measuring area was recorded using a high-speed camera at a resolution of 1280 × 1024 pixels and a frame rate of 1000 fps. Prior to bubble generation, a ruler was placed in the middle of the tank and perpendicular to the camera lens to record the calibration of the gas bubble diameter dimensions. To avoid the influence of other bubble movements and wake vortices on the measurement results, videos with only one gas bubble in tank were used for data processing. The collected video

data were analyzed using a data acquisition software and an image digital analysis software. Fig. 2 presented the processing steps of sequence gas bubble rising images. The raw image was processed from Fig. 2 (a) to Fig. 2 (d). The major semi-axes of the ellipse fitted onto bubble area was defined as a, and the minor semi-axis was defined as b. The bubble aspect ratio (A_R) was calculated by equation: $A_R = b/a$. As shown in Fig. 2 (e), the bubble centroid coordinates for each frame were used for bubble velocity (v) [33]: $v=\sqrt{(x_{t+\Delta t}-x_t)^2+(y_{it+\Delta t}-y_t)^2}/\Delta t$, where ($x_t$, y_t) and ($x_{t+\Delta t}$, $y_{t+\Delta t}$) were the geometric center position coordinates of the bubble at time t and $t + \Delta t$, respectively. Δt is the interval between two adjacent frames, and set as 0.001 s in this study.

2.3. Surface tension measurement

An A60 surface tension analyzer (USA KINO Industry Co., Ltd., USA) was used to measure the surface tension using the platinum plate method. Before each experiment, the platinum plate was rinsed with deionized water and heated with an alcohol lamp to remove impurities. Subsequently, a sample of 50 mL solution was poured into glassware, which was placed on the sample plate. The chilled platinum plate was fixed on the balance hook, and then contacted with measured solution. Each surface tension measurement was thrice performed, and the average value and error were obtained as the reported data.

2.4. Viscosity measurement

An NDJ-8S rotational viscometer (Shanghai Hengping Instrument Co., Ltd., China) was used to measure the viscosity of simple solution. Before each experiment, the rotor was rinsed with deionized water and measured solution. In the experiment, a 20 mL of sample solution was poured into measuring tube. Subsequently, a rinsed rotor was fixed in the insulation cover of the instrument and immersed in the measuring solution. The viscosity was measured repeatedly until the displayed value remain constant within ± 0.1 s, then the average value was reported. Each measurement was carried out three times, and the average value and error were reported as the final data.

2.5. Sound field simulation

The sound field was investigated by solving the Helmholtz equation using COMSOL Multiphysics 5.6 software. Calculation using coupled acoustic-structural physical fields studied in the frequency domain. The parameters required in the simulation are shown in Table 1. Fig. 3 (a) shows the geometry of the ultrasonic experimental system. The transducer was stacked by 4 layers of piezoelectric ceramic rings pieces. Fig. 3(b) shows the boundary condition setting of the system. The boundary I was the contact surface between the ultrasonic horn tip and the liquid, which was set as the acoustic structure coupling boundary. The liquid was in contact with the air and the sound waves were totally reflected. Therefore, the boundary II was set as a soft sound field boundary. The ultrasound horn was 21 cm from the bottom of tank (H_2) and the height of the solution in the tank, H_1 is 23 cm. Fig. 3(c) shows the tetrahedral mesh of the ultrasonic experimental system. In order to ensure the computational accuracy, the region mesh needs to ensure that there are at least 6 meshes in one wavelength, i.e., the size of the largest cell of the mesh is 12.5 mm. The number of tetrahedral meshes is 27,999, the number of mesh vertices is 11,909, and the minimum mesh mass is 0.03674, which is enough for the requirements of acoustic meshing.

3. Results

3.1. Bubble rise trajectory analysis

Fig. 4 shows eight typical 2D image sequences of the bubble upward path. As shown in Fig. 4 (a)-(d), the gas bubble rose in a zigzag trajectory, and the shape showed alternating changes of flat ellipse and ellipse. This change of the bubble shape broke the force balance of the gas bubble, resulting in the gas bubble being in an unstable state, which promoted the shift of bubble rise trajectory. The offset of the bubble on the X axis decreased slightly with an increase in MIBC concentration, which was not related to the presence of ultrasonication, indicating that the addition of MIBC might reduce the fluctuation of the bubble trajectory and promote it to be stabler. Fig. 4 (e)-(h) presents the typical image sequences of the gas bubble upward path with the ultrasonication. A gas bubble was observed to be almost spherical with ultrasonication. At any experimental MIBC concentrations, the bubble X-axis offset with ultrasonication was smaller than that without ultrasonication, indicating that ultrasonication could stabilize the bubble motion, even at low MIBC concentrations. Besides, the gas bubble exhibited an irregular zigzag trajectory, different from it without ultrasonication, caused by the uneven distribution of energy produced using the ultrasound horn.

3.2. Effect of ultrasonication on bubble aspect ratio

The bubble average aspect ratio with and without ultrasound are presented in Fig. 5. In the experimental MIBC concentration range, the bubble aspect ratio was observed to increase as the MIBC concentration increased, independent of the presence of ultrasound. This phenomenon implied that the bubble shape tended to be spherical at a high MIBC concentration. The increase in MIBC concentration changed the surface tension of solution, the deformation of the bubble is counteracted by the surface tension, thus the gas bubble tends to restore the spherical shape [20]. Bubble aspect ratio with ultrasound was appreciably larger than that without ultrasound at the same MIBC concentration, and the ultrasonication had a more significant influence on bubble aspect ratio at a low concentration than high concentration. The bubble instantaneous aspect ratio as a function of time in 0.157 mmol/L MIBC solution is shown in the inset of Fig. 5. The bubble aspect ratio was observed to fluctuate periodically over time without ultrasonication, and the period and the amplitude of change were approximately 90 ms and 0.4, respectively. With the ultrasonication, the bubble aspect ratio gradually increased with time increasing, until it reached a maximum of 0.8 at 120 ms, and then varied irregularly in a small range around 0.75, which implied that ultrasonication could destroy the periodic change of the bubble aspect ratio. It is worth noting that the instantaneous aspect ratio of the bubble with ultrasound was overall higher than that without ultrasound, indicating the ultrasound positively affected on the bubble aspect ratio in any rising state.

3.3. Effect of ultrasonication on bubble velocity

Fig. 6 presents bubble average velocity in the absence and presence of the ultrasonication. In the experimental range of the MIBC concentration, the bubble average velocity decreased with its increase. This behavior has been reported by Finch et al. [34], the high surface gradients and great Gibbs elasticity caused by the increase of MIBC addition resulted from the effect of concentration on bubble velocity[18]. At the same concentration of MIBC solution, the bubble rising velocity with ultrasonication was significantly smaller than that without ultrasonication. It indicated that

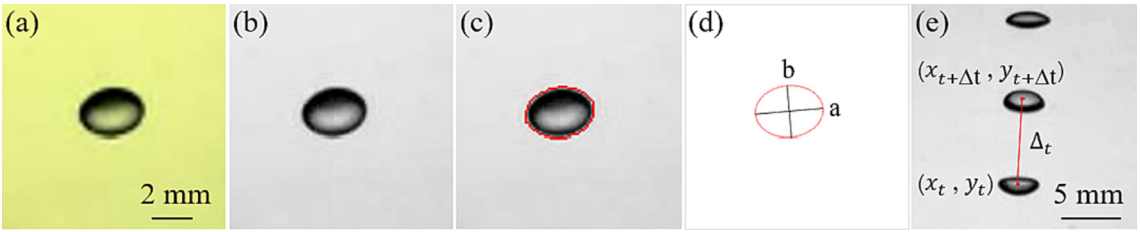

Fig. 2. Image processing steps in Image Pro Plus software: (a) raw image, (b) background subtraction, (c) ellipse fitting, (d) shape detection, (e) velocity analysis.

Table 1
Parameters used in the simulation.

Name	value	Unit
Ultrasound frequency	20	kHz
Density of liquid	998	kg/m^3
Sound velocity of liquid	1500	m/s
Density of acrylic	1200	kg/m^3
Sound velocity of acrylic	2670	m/s

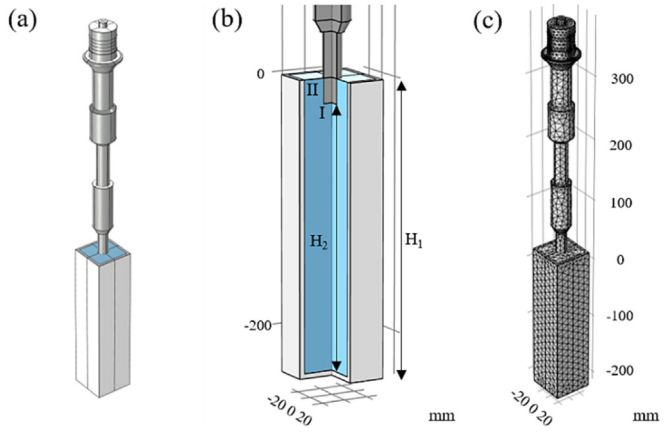

Fig. 3. Numerical model: (a) geometrical model, (b) boundary setting, (c) mesh meshing model.

ultrasonication can slow down the bubble rising velocity and prolong the time of gas bubble stays in the pulp, thus resulting in an increase of gas holdup, which is beneficial for flotation. Besides, the variation in MIBC concentration had a significant influence on the bubble velocity in the absence of ultrasonication, and it

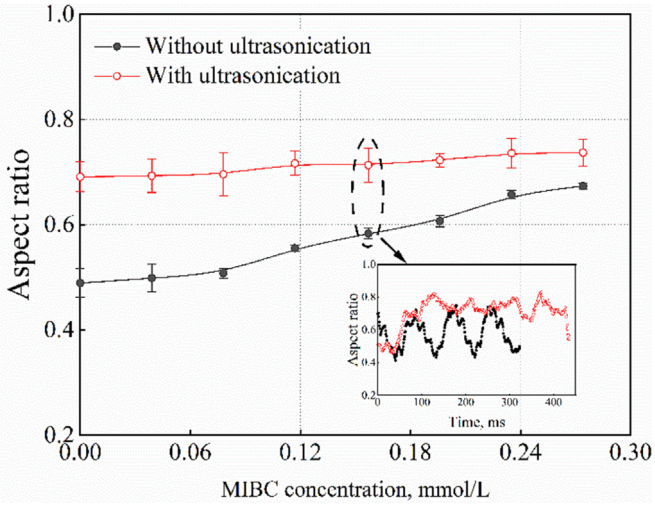

Fig. 5. The aspect ratio as functions of MIBC concentrations in the absence and presence of ultrasonication.

had a little effect on bubble rising velocity at the presence of ultrasonication. The illustration in Fig. 6 shows the bubble instantaneous velocity as a function of time in 0.157 mmol/L MIBC solution. As noted, without ultrasonication, the bubble velocity changed periodically over time with a period of approximately 90 ms, which was identical to that of the bubble aspect ratio, and the amplitude was 120 mm/s. The ultrasonication was found to destroy the periodic fluctuation of the bubble velocity. The bubble rising velocity decreased with time until it increased after 300 ms, then rapidly decreased after 400 ms. In any experimental time, the instantaneous bubble velocity with ultrasound was almost smaller than that without ultrasound.

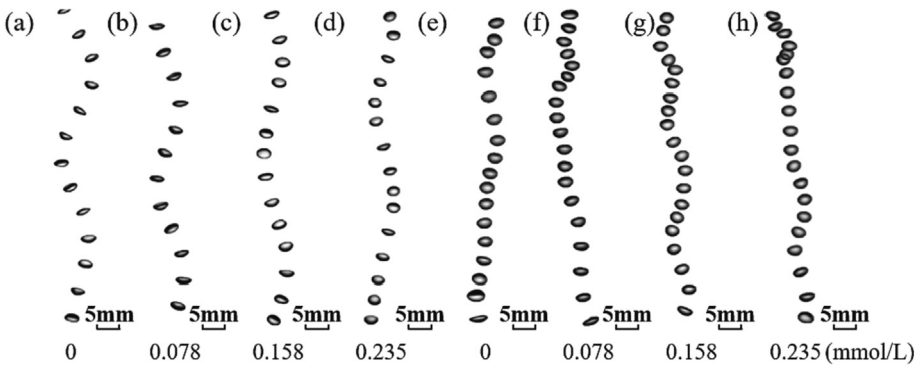

Fig. 4. Image sequences of bubble rise process in different concentrations of MIBC solutions, (a)-(d) without ultrasonication; (e)-(h) with ultrasonication. The time interval between two consecutive bubbles was 25 ms.

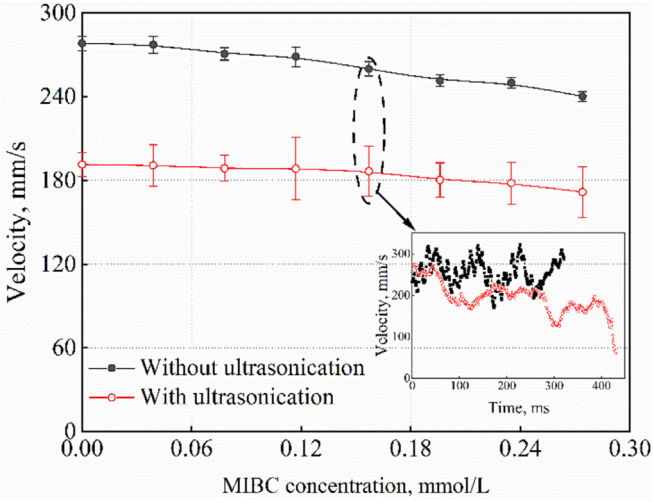

Fig. 6. The velocity as functions of MIBC concentration in the absence and presence of ultrasonication.

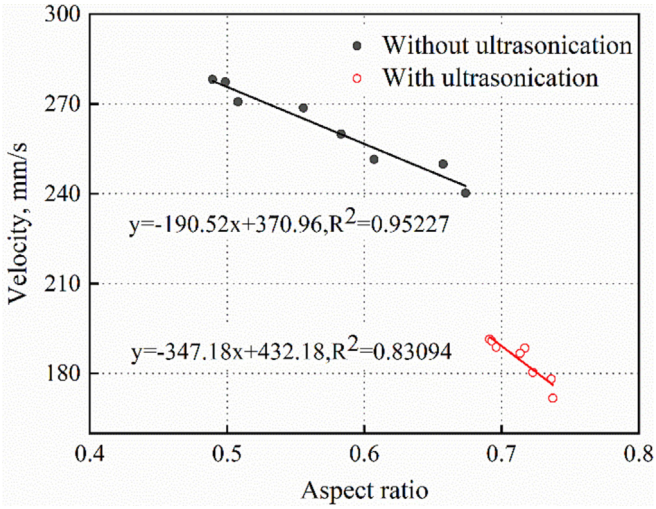

Fig. 7. Bubble average velocity vs bubble aspect ratio.

3.4. Relationship between aspect ratio and velocity

Fig. 7 summarizes the bubble velocity as a function of aspect ratio for MIBC various concentrations in the range of tested conditions. A roughly linear relationship between bubble average velocity and aspect ratio was observed, which was not associated with the MIBC concentration. Therefore, it was considered that both the bubble shape and velocity were affected by similar mechanisms, i. e. the Gibbs elastic force at the top of the bubble [35]. Combined with drag coefficient proposed by Moore [36] considering the dimensionless number about bubble deformations (W_e, Weber number), a negative correlation was found between the W_e number and bubble aspect ratio. Since, the W_e is negatively correlated with drag coefficient, the drag coefficient and aspect ratio are positively correlated. It indicated that the higher the bubble sphericity, the higher the drag coefficient, thus reducing the bubble rising velocity, which is consistent with our experimental data. In fact, the drag coefficient is not only related to the bubble shape, but also related to a variety of factors such as the solution surface tension, viscosity, fluid flow et al. The slope between the bubble velocity and aspect ratio without ultrasound was smaller than that with ultrasound, implying that the ultrasonication could strengthen the effect of the bubble aspect ratio on the velocity. However, the fitted line with ultrasound had a smaller R^2 value, indicating the ultrasound increased the disorder of bubble characteristics within the system.

4. Discussion

4.1. Mechanism of surfactant action in rising bubble

As shown in Fig. 8 (a), usually, in pure water systems, there is no surface-active substances present on the bubble interface, so the bubble surface is fully mobile, and thus the gas inside bubbles can internally circulate. This reduces friction between the rising gas bubble and the liquid surrounding the gas bubble, which results in the reduction coefficient of resistance, hence gas bubbles rise the fastest [37]. Moreover, during gas bubble rises, the gas bubble is subjected to drag and buoyancy forces, and the pressure difference between the upper and lower surfaces of the gas bubble induces an upward jet, thereby the bubble deformation is triggered. This changes the bubble projected area, which affects the bubble velocity [38–40]. As noted in Fig. 8 (b), in surfactant solutions, surface active substances present at the bubble interface to

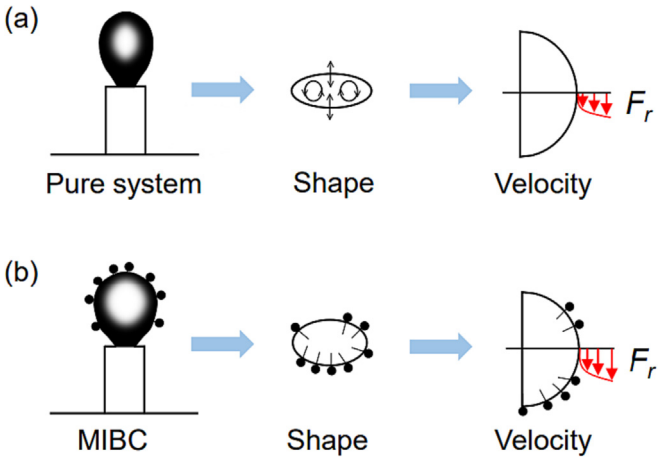

Fig. 8. Scheme of rising gas bubbles with: (a) water and (b) MIBC solutions with the effect on the bubble shape and velocity.

form a certain fixed surface, which inhibits internal circulation at the bubble surface, thus resulting in an increased drag coefficient. Furthermore, as the gas bubble rises, water flows over the bubble surface, some MIBC molecules are swept to the bottom of the gas bubble, and the surface tension of the bubble bottom is reduced, resulting in a surface gradient between the top and bottom of the gas bubble, then leading to Marangoni shear stress. The Marangoni shear stress acts in the opposite direction to the pressure difference between the upper and lower surfaces of the gas bubble, thus prevents the gas bubble from deforming and slows the gas bubble rise [38,41]. Thus, bubble rising velocity in surfactant solutions is much smaller than that of gas bubble in the same volume equivalent diameter in a pure system. The Marangoni shear stress is closely related to the reagent addition. Generally, a higher MIBC addition leads to higher surface gradients and a greater Marangoni shear stress, which explains why the bubble aspect ratio increases and bubble velocity decreases with increasing MIBC concentration.

4.2. Effect of ultrasonication on solution properties

The same action as surfactant, ultrasound stabilizes the bubble shape and decreases bubble rising velocity. It needs to be determined that whether the contribution of ultrasound on the bubble rising behavior can be attributed to the effect of ultrasound

on the properties of the solution. Surface tension and viscosity of the solution are common properties that affect bubble characteristics. Fig. 9 (a) and (b) show the effect of ultrasound on the surface tension and viscosity of the experimental solutions. The surface tension and viscosity of MIBC solution decreased and increased respectively with the increase of MIBC concentrations, which barely relates to the presence of ultrasonication. The concentration-surface tension curves with and without ultrasonication were similar. At the same experimental MIBC concentration, the surface tension of MIBC solutions without ultrasonication is slightly different from that of solutions with ultrasonication. The same is for the viscosity of the solution. Notably, considering the effect of ultrasonication on the surface tension and viscosity of the MIBC solution and changes in bubble behavior with and without ultrasonication together, the effect of ultrasonication on MIBC solution properties seems not to be strong enough to influence bubble rising behavior to the extent in Fig. 5 and Fig. 6.

4.3. Mechanism of ultrasonication in rising bubble

It has been shown that surfactants regulate bubble velocity by controlling surface tension to influence bubble shape [16,17]. However, the correlation between bubble shape and bubble velocity was significantly reduced in the presence of ultrasonication. Therefore, the effect of ultrasound on the bubble movement speed did not only depend on its influence on the bubble shape. There are three points that may be considered in seeking the explanations for the effect of ultrasonication on the bubble rising characteristics.

The first possibility is the presence of the bubble surface waves. The gas bubble could undergo different oscillations driven by the acoustic pressure fluctuations. At low sound pressure, the gas bubble could undergo volume (or breathing) oscillations. When the sound pressure exceeds the threshold (minimum acoustic condition causes a change in the bubble behavior), the bubble surface gradually develops into the shaped oscillation with many surface wave modes with the sound pressure rising, and then becomes highly disordered until collapse. Therein, the shaped oscillation mode at lowest is the Faraday wave, which present regular geometric distortions [42–44]. Fig. 10 (a)-I and (III) show gas bubbles in pure water and MIBC solution for reference. In pure water and MIBC solution, the surface of the observed bubbles was flat. At the same solution conditions, the gas bubble in the presence of ultrasonication exhibited violent nonlinear vibrations, i.e., surface pulsation. Fig. 10 (a)- II and (IV) show the details of the bubble sur-

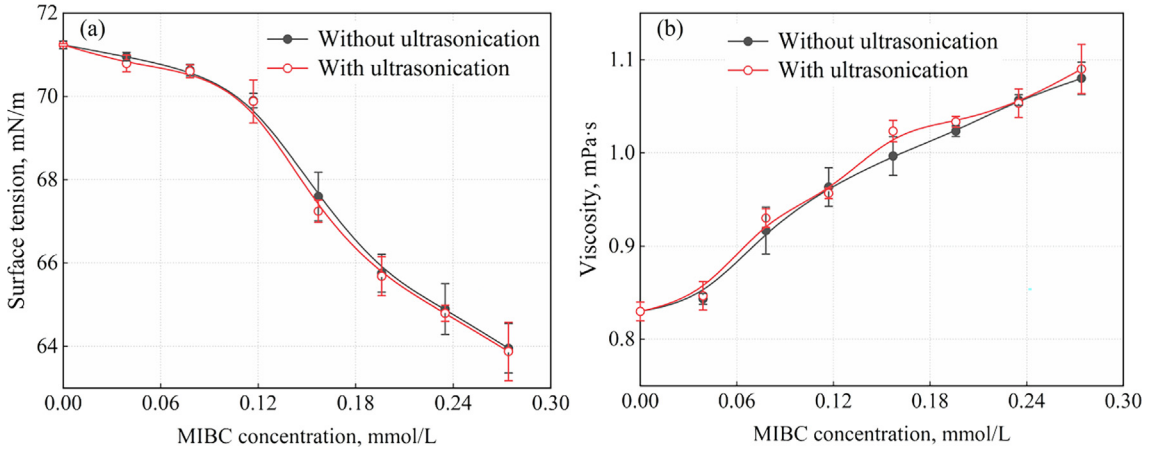

Fig. 9. Solution surface tension (a) and viscosity (b) as a function of MIBC concentration. (The shear rate for viscosity measurements is 73.44 s^{-1}).

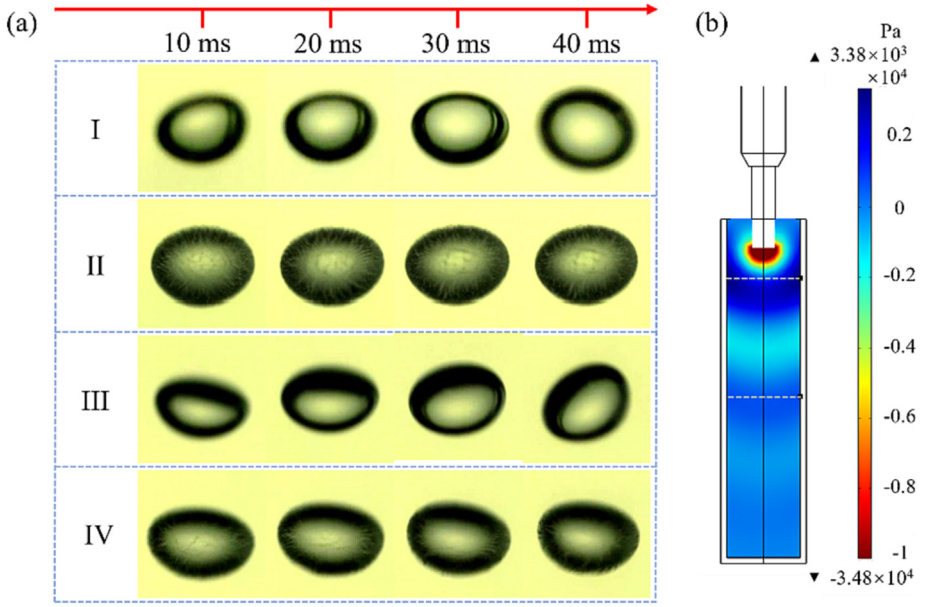

Fig. 10. (a) Rising gas bubble surface in different condition: (I) with water; (II) with water and ultrasonication; (III) with MIBC solution; (IV) with MIBC solution and ultrasonication. (b) The sound field in the observation tank.

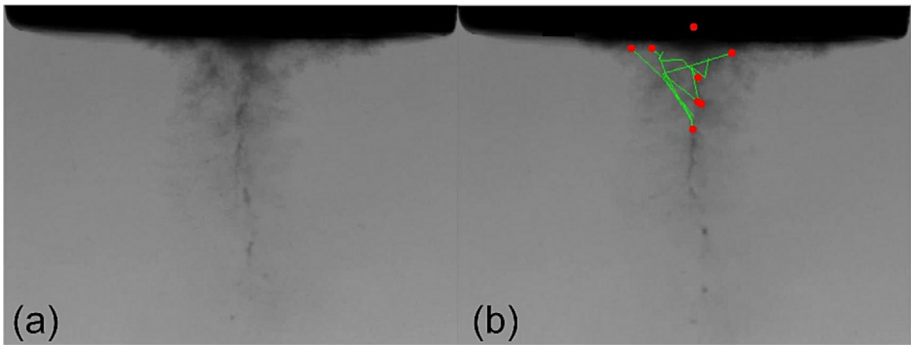

Fig. 11. Cavitation bubbles generated by ultrasonic horn at 20 kHz and 90 W in frequency and output power, observed by the high-speed camera. The picture b is the analysis of the cavitation bubble behaviors recorded from the picture a to that at 18 ms later. The small red circles are the starting points for cavitation bubble motion and the green curves indicate the calculated streamlines of bubbles. (For interpretation of the references to colour in this figure legend, the reader is referred to the web version of this article.)

face oscillations. The bubble surface was deformed, but not in clear periodic and regular shape oscillatory, which indicated that several surface wave forms are superimposed on the bubble surface. To better analyze the bubble surface waves, during gas bubble rising process, the COMSOL software was used to calculated the sound filed. The sound field in the observation tank is shown in Fig. 10 (b). The ultrasound was not uniformly distributed in the experimental tank, but the acoustic pressure did not decrease with far away from the ultrasonic probe. Rather, there are high and low acoustic pressure regions alternating distribution, which is due to the reflective effect of the walls of the tank. The observation area is the dashed area in Fig. 10 (b). Theoretically, the gas bubble initially appeared in the positive sound pressure region, then moved upward into the negative sound pressure region, and then crossed the negative sound pressure region into the positive sound pressure region. The acoustic pressure on the bubble surface varies during the bubble rising process, thus the bubble experiences multiple oscillation. Dangla and Poulain have proved that the Faraday wave on bubble surface can reduce the bubble rising velocity [45]. It is possible that the superposition of multiple surface waves could reduce the bubble rising velocity. Like Faraday wave, when the bubble departs the spherical geometry, the shape-dependent drag coefficient always increases, so the average drag coefficient also increases, which will reduce the bubble velocity [45]. Furthermore, other mechanisms cannot be ignored. For example, the surface wave enhances the acoustic flow [46], which will affect the bubble shape [47] and thus the bubble velocity. Moreover, the bubble surface oscillations enhance the flow field fluctuations at the bubble surface, and the flow field fluctuations are mainly located near the bubble surface with additional micro vortices [48]. This also has the potential to reduce the bubble motion velocity.

The second relates to the acoustic cavitation bubble motion. In the experiment, the influence from other small bubbles is impossible to eliminate. When ultrasonic horn operates, the ultrasonic horn generates massive small bubbles owing to the effect of acoustic cavitation. Fig. 11 (a) and (b) show the cavitation bubble behaviors around ultrasonic horn. The small red circles were the starting points for cavitation bubble motion and the green curves indicated the calculated streamlines of cavitation bubbles. This illustrated that some small bubbles formed bubble clouds and upward to the horn tip, and some moved away from the horn tip [49] and around the observed gas bubble, which was consistent with the study of Yasui et al. [50]. The cavitation bubbles moved irregularly around the observed gas bubble and the flow lines of the cavitation bubbles changed sharply with time, which caused violent disturbance around the observed gas bubble. It is possible that the cavitation bubble increases the bubble aspect ratio and decreases the bubble rising velocity by influencing the flow field around gas bubble.

The third possible explanation is that the shape and velocity of the observed gas bubble are influenced by the acoustic radiation pressure. Owing to the nonlinear effect of ultrasound, the acoustic radiation pressure originates from the pressure gradient around the bubble [29]. As shown in Fig. 10 (b), the sound pressure around the gas bubble was constantly changing during the bubble rising, thus the acoustic radiation pressure (P_A) around the gas bubble constantly changed. It has been shown that the negative P_A around gas bubble indicates the suction effect on gas bubble and positive P_A means compression effect on the gas bubble [51,52]. Therefore, the velocity of the gas bubble could be influenced by the combined forces in the vertical direction of the acoustic radiation pressure, while the bubble shape could be influenced by combined forces in the horizontal and vertical directions of the acoustic radiation pressure. Moreover, acoustic streaming of the Rayleigh type caused by cavitation bubble streaming was induced in solution [53]. Acoustic streaming, which behaves as a kind of integral flow and inevitably affects the movement of bubbles [54]. Therefore, it is possible that ultrasonication affects bubble rising behaviors due to Rayleigh streaming.

5. Conclusion

In this paper, bubble rising characteristics at different MIBC concentrations with or without ultrasonication were explored using a laboratory visualization system of bubble motion and the possible mechanisms of ultrasound action were explored. This study may provide new insights into the application of ultrasonication in mineral flotation separation. Bubble aspect ratio was found to increase with the increasing surfactant concentrations, but the rising velocity was in opposite state. In the same MIBC concentration, the addition of ultrasound reduced the deformation and rising velocity of the bubble. A roughly negative linear relationship between bubble average velocity and aspect ratio was observed. Three perspectives were proposed in seeking the explanation for the effect of ultrasonication on the bubble rising characteristics: (1) bubble surface waves affect bubble characteristics by changing the bubble shape and inducing additional micro-vortices around the gas bubble surface. (2) The vibration of cavitation bubbles could influence gas bubble motion by inducing a certain perturbation effect on the surrounding environment of the rising gas bubble. (3) Acoustic radiation pressure affects gas bubble motion by changing the force on the gas bubble.

Declaration of competing interest

The authors declare that they have no known competing financial interests or personal relationships that could have appeared to influence the work reported in this paper.

Acknowledgment

This work had received the financial support from the National Natural Science Foundation of China (No. 52225405, No. U21A20325) and Graduate Innovation Program of China University of Mining and Technology (2023WLKXJ079), and all authors express their sincere thanks for them.

References

[1] C.Q. Wang, H. Wang, J.G. Fu, Y.N. Liu, Flotation separation of waste plastics for recycling-A review, Waste Manag. 41 (2015) 28–38.
[2] M.K. Nazir, L. Dyer, B. Tadesse, B. Albijanic, N. Kashif, Flotation performance of calcined spodumene, Adv. Powder Technol. 33 (2022) 103772.
[3] G.Z. Kyzas, K.A. Matis, Flotation in Water and Wastewater Treatment, Processes 6 (2018) 16.
[4] H. Wang, W. Yang, X. Yan, L. Wang, Y. Wang, H. Zhang, Regulation of bubble size in flotation: A review, J. Environ. Chem. Eng. 8 (2020) 104070.
[5] B. Shahbazi, B. Rezai, S.M.J. Koleini, Bubble-particle collision and attachment probability on fine particles flotation, Chem. Eng. Process.-Process Intensification 49 (2010) 622–627.
[6] S. Chen, Z. Li, N. Zhang, L. Liu, J. Qu, Y. Yu, J. Chang, Z. Zhu, X. Tao, A novel method for evaluating the hydrophobic interaction between coal particles and air bubbles and its role in flotation, Adv. Powder Technol. 33 (2022) 103484.
[7] S. Ata, Phenomena in the froth phase of flotation — A review, Int. J. Miner. Process. 102–103 (2012) 1–12.
[8] Y.S. Cho, J.S. Laskowski, Effect of flotation frothers on bubble size and foam stability, Int. J. Miner. Process. 64 (2002) 69–80.
[9] R.A. Grau, J.S. Laskowski, K. Heiskanen, Effect of frothers on bubble size, Int. J. Miner. Process. 76 (2005) 225–233.
[10] Y.H. Tan, J.A. Finch, Frother structure-property relationship: Effect of alkyl chain length in alcohols and polyglycol ethers on bubble rise velocity, Miner. Eng. 95 (2016) 14–20.
[11] S.S. Khaleduzzaman, I.M. Mahbubul, I.M. Shahrul, R. Saidur, Effect of particle concentration, temperature and surfactant on surface tension of nanofluids, Int. Commun. Heat Mass Transfer 49 (2013) 110–114.
[12] R. Alam, J.Q. Shang, A.H. Khan, Bubble size distribution in a laboratory-scale electroflotation study, Environ. Monit. Assess. 189 (2017) 193.
[13] Z.H. Chen, S. Ata, G.J. Jameson, Behaviour of bubble clusters in a turbulent flotation cell, Powder Technol. 269 (2015) 337–344.
[14] D. Li, H. Wang, L. Yang, X. Yan, L. Wang, H. Zhang, Intensification effects of stirred fluid on liquid?solid, gas?liquid and gas?solid interactions in flotation: A review, Chemical Engineering and Processing-Process Intensification 152 (2020) 107943.
[15] M. Krzan, K. Malysa, Profiles of local velocities of bubbles in n-butanol, n-hexanol and n-nonanol solutions, Colloids and Surfaces a-Physicochemical and Engineering Aspects 207 (2002) 279–291.
[16] W. Kracht, J.A. Finch, Effect of frother on initial bubble shape and velocity, Int. J. Miner. Process. 94 (2010) 115–120.
[17] M. Maldonado, J.J. Quinn, C.O. Gomez, J.A. Finch, An experimental study examining the relationship between bubble shape and rise velocity, Chem. Eng. Sci. 98 (2013) 7–11.
[18] H. Zhu, A.L. Valdivieso, J. Zhu, F. Min, S. Song, D. Huang, S. Shao, Effect of dodecylamine-frother blend on bubble rising characteristics, Powder Technol. 338 (2018) 586–590.
[19] X. Yan, Y. Jia, L. Wang, Y. Cao, Drag coefficient fluctuation prediction of a single bubble rising in water, Chem. Eng. J. 316 (2017) 553–562.
[20] X. Yan, K. Zheng, Y. Jia, Z. Miao, L. Wang, Y. Cao, J. Liu, Drag Coefficient Prediction of a Single Bubble Rising in Liquids, Ind. Eng. Chem. Res. 57 (2018) 5385–5393.
[21] S.D. Barma, Ultrasonic-assisted coal beneficiation: A review, Ultrason. Sonochem. 50 (2019) 15–35.
[22] Y. Mao, W. Xia, Y. Peng, G. Xie, Ultrasonic-assisted flotation of fine coal: A review, Fuel Process. Technol. 195 (2019) 106150.
[23] W. Wang, N. Zhang, Flotation bubble size distribution rules with ultrasonic radiation, Journal of MInging, Sci. Technol. 3 (2018) 84–90.
[24] S.G. Ozkan, Further Investigations on Simultaneous Ultrasonic Coal Flotation, Minerals 7 (2017) 177.
[25] D. Yasmin, S. Mitra, G.M. Evans, Analysis of dynamic interactions in a bubble-particle system in presence of an acoustic field, Miner. Eng. 131 (2019) 111–123.
[26] L.X. Yang, F.S. Xu, Q. Zhang, Z.K. Liu, G.W. Chen, Gas -liquid hydrodynamics and mass transfer in microreactors under ultrasonic oscillation, Chem. Eng. J. 397 (2020) 125411.
[27] K.D. Gao, H. Liu, L.Q. Sun, Z.H. Zhang, Effect of Gas Input Conditions and Ultrasound on the Dynamic Behavior of Flotation Bubbles, ACS Omega 7 (2022) 22326–22340.
[28] M. Ashokkumar, The characterization of acoustic cavitation bubbles - An overview, Ultrason. Sonochem. 18 (2011) 864–872.
[29] Y. Chen, V.N.T. Truong, X. Bu, G. Xie, A review of effects and applications of ultrasound in mineral flotation, Ultrason. Sonochem. 60 (2020) 104739.
[30] Y. Mao, X. Bu, Y. Peng, F. Tian, G. Xie, Effects of simultaneous ultrasonic treatment on the separation selectivity and flotation kinetics of high-ash lignite, Fuel 259 (2020) 116270.
[31] Y. Mao, Y. Chen, X. Bu, G. Xie, Effects of 20 kHz ultrasound on coal flotation: The roles of cavitation and acoustic radiation force, Fuel 256 (2019) 115938.
[32] X.J. Ma, T.Y. Xing, B. Huang, Q.H. Li, Y.F. Yang, Combined experimental and theoretical investigation of the gas bubble motion in an acoustic field, Ultrason. Sonochem. 40 (2018) 480–487.
[33] Z. Tian, Y. Cheng, X. Li, L. Wang, Bubble shape and rising velocity in viscous liquids at high temperature and pressure, Exp. Therm Fluid Sci. 102 (2019) 528–538.
[34] J.A. Finch, J.E. Nesset, C. Acuña, Role of frother on bubble production and behaviour in flotation, Miner. Eng. 21 (2008) 949–957.
[35] J.J. Quinn, M. Maldonado, C.O. Gomez, J.A. Finch, Experimental study on the shape-velocity relationship of an ellipsoidal bubble in inorganic salt solutions, Miner. Eng. 55 (2014) 5–10.
[36] D.W. Moore, The Rise of a Gas Bubble in a Viscous Liquid, J. Fluid Mech. 6 (1959) 113–130.
[37] P. Pawliszak, V. Ulaganathan, B.H. Bradshaw-Hajek, R. Manica, D.A. Beattie, M. Krasowska, Mobile or Immobile? Rise Velocity of Air Bubbles in High-Purity Water, Journal of Physical Chemistry C 123 (2019) 15131–15138.
[38] K. Laqua, K. Malone, M. Hoffmann, D. Krause, M. Schlüter, Methane bubble rise velocities under deep-sea conditions—Influence of initial shape deformation, Colloids Surf A Physicochem Eng Asp 505 (2016) 106–117.
[39] W. Li, Jiao Shouhua, Tang Ke, Yang Yiang, Qu Wenhai, Chai Xiang, Experimental investigation on characteristic of single bubble motion in stagnant water, Atomic Energy Sci. Technol. 54 (2020) 1652–1659.
[40] H. Wang, Z.Y. Zhang, Y.M. Yang, Y. Hu, H.S. Zhang, Numerical investigation of the deformation mechanism of a bubble or a drop rising or falling in another fluid, Chin. Phys. B 17 (2008) 3847–3855.
[41] S. Takagi, Y. Matsumoto, Surfactant Effects on Bubble Motion and Bubbly Flows, Annu. Rev. Fluid Mech. 43 (2011) 615–636.
[42] Z.Y. Dong, C.Q. Yao, Y.C. Zhang, G.W. Chen, Q. Yuan, J. Xu, Hydrodynamics and mass transfer of oscillating gas-liquid flow in ultrasonic microreactors, AIChE J 62 (2016) 1294–1307.
[43] D.G. Offin, P.R. Birkin, T.G. Leighton, Electrodeposition of copper in the presence of an acoustically excited gas bubble, Electrochem. Commun. 9 (2007) 1062–1068.
[44] F. Prabowo, C.D. Ohl, Surface oscillation and jetting from surface attached acoustic driven bubbles, Ultrason. Sonochem. 18 (2011) 431–435.
[45] R. Dangla, C. Poulain, When sound slows down bubbles, Phys. Fluids 22 (2010).
[46] A.O. Maksimov, Viscous streaming from surface waves on the wall of acoustically-driven gas bubbles, European Journal of Mechanics B-Fluids 26 (2007) 28–42.
[47] Z. Chen, D.Y. Zang, L. Zhao, M.F. Qu, X. Li, X.G. Li, L.X. Li, X.G. Geng, Liquid Marble Coalescence and Triggered Microreaction Driven by Acoustic Levitation, Langmuir 33 (2017) 6232–6239.
[48] F.S. Xu, L.X. Yang, Z.K. Liu, G.W. Chen, Numerical investigation on the hydrodynamics of Taylor flow in ultrasonically oscillating microreactors, Chem. Eng. Sci. 235 (2021).
[49] T. Nowak, C. Cairos, E. Batyrshin, R. Mettin, Acoustic Streaming and Bubble Translation at a Cavitating Ultrasonic Horn, 20th International Symposium on Nonlinear Acoustics (ISNA) including the 2nd International Sonic Boom Forum (ISBF)Ecole Centrale Lyon, Lyon, France, 2015.
[50] K. Yasui, Y. Iida, T. Tuziuti, T. Kozuka, A. Towata, Strongly interacting bubbles under an ultrasonic horn, Phys. Rev. E 77 (2008) 016609.
[51] D. Zang, Y. Yu, Z. Chen, X. Li, H. Wu, X. Geng, Acoustic levitation of liquid drops: Dynamics, manipulation and phase transitions, Adv. Colloid Interface Sci. 243 (2017) 77–85.
[52] D. Zang, J. Li, Z. Chen, Z. Zhai, X. Geng, B.P. Binks, Switchable Opening and Closing of a Liquid Marble via Ultrasonic Levitation, Langmuir 31 (2015) 11502–11507.
[53] S. Nomura, K. Murakami, Y. Sasaki, Streaming Induced by Ultrasonic Vibration in a Water Vessel, Jpn. J. Appl. Phys. 39 (2000) 3636–3640.
[54] W. Wu, P. Yang, W. Zhai, B. Wei, Oscillation and Migration of Bubbles within Ultrasonic Field, Chin. Phys. Lett. 36 (2019) 084302.